BioNanoScience (2025) 15:317
https://doi.org/10.1007/s12668-025-01932-4

REVIEW

Engineered Nanoparticles Enhance Photodynamic Inactivation Against the WHO Fungal Priority Pathogens. A Systematic Review

Abdênego R. da Silva[1] · Bruno L. Raposo[1] · Geyse S. de Lima[2] · Jacqueline C. Bueno-Janice[2] · Fábio P. Sellera[3,4] · Paulo E. Cabral Filho[2] · Adriana Fontes[2] · Martha S. Ribeiro[1]

Accepted: 7 April 2025 / Published online: 10 April 2025

Abstract

Fungal infections pose a significant global health concern, prompting the WHO to prioritize fungi needing novel therapies. Photodynamic inactivation (PDI), which uses light, a photosensitizer (PS), and oxygen to produce oxidative stress, has shown promising results against fungi. Engineered nanoparticles (NPs) have emerged as a promising ally to enhance PDI. This systematic review examined the combined effects of PDI and NPs on the WHO's priority fungal pathogens. After screening Embase, Pubmed, Scopus, and Web of Science, ten studies were selected based on criteria including consistent NP characterization, PDI protocol, and a focus on critical and high priority fungi. Most studies targeted *Candida albicans*, with only one of them on *Fusarium keratoplasticum*. Only 4 studies reported the effects of PDI mediated by NPs on biofilms. Nanostructures applied included metallic, superparamagnetic iron oxide, micelle, and polymeric NPs. Findings indicate that i-) NPs can enhance the solubility of PSs by carrying hydrophobic compounds; ii-) NPs may improve the chemical stability of PSs avoiding aggregation, which could reduce the PS performance; iii-) NPs can be engineered to reduce the required PS concentration for effective fungal elimination, and iv-) Metallic NPs can improve the photophysical properties of PSs, such as enhancing the generation of reactive oxygen species by localized surface plasmon resonance. Further research is needed to extend these findings beyond in vitro conditions.

Keywords Biofilm · *Candida albicans* · *Fusarium keratoplasticum* · Lasers · LEDs · Nanostructures · Photosensitization

1 Introduction

Fungal infections have become a significant global health threat, causing rising morbidity and mortality, especially among vulnerable populations [1]. In this regard, their clinical impacts on individuals with weakened immune systems, such as those with HIV/AIDS, transplant recipients, and patients undergoing chemotherapy, are concerning [2].

Recognizing the urgent need to address the burden of fungal diseases, the World Health Organization (WHO) published a list of priority fungal pathogens in October 2022 [3]. This list identifies 19 fungal species, stratified into three groups (critical, high, and medium priority), that pose the greatest threat to public health and aims to guide research, surveillance, and resource allocation to tackle these infections effectively [3]. The selected fungi were ranked based on their ability to cause life-threatening infections (*e.g.,* invasive candidiasis, aspergillosis, cryptococcal meningitis, and other systemic mycoses), limited therapeutic options, and their potential for development of drug resistance. Taking this into account, there is a pressing

Abdênego R. da Silva, Bruno L. Raposo, Geyse S. de Lima, Jacqueline C. Bueno-Janice, Fábio P. Sellera, Paulo E. Cabral Filho, Adriana Fontes and Martha S. Ribeiro contributed equally to this work.

✉ Martha S. Ribeiro
marthasr@usp.br

[1] Center for Lasers and Applications, Energy and Nuclear Research Institute (IPEN-CNEN), Av. Lineu PrestesCidade Universitária, São Paulo, SP 2242, 05508 - 000, Brazil

[2] Department of Biophysics and Radiobiology, Federal University of Pernambuco, Recife, PE, Brazil

[3] School of Veterinary Medicine, Metropolitan University of Santos, Santos, SP, Brazil

[4] Department of Internal Medicine, School of Veterinary Medicine and Animal Science, University of São Paulo, São Paulo, Brazil

need to search for novel, effective therapeutic options to combat this emerging public health problem.

Antimicrobial photodynamic therapy (APDT) represents a promising approach against microbial infections since it possesses broad-spectrum activity against several clinically important pathogens, including fungal agents [4]. APDT or photodynamic inactivation (PDI, a term usually used for in vitro studies) combines a light source of specific wavelength, a photosensitizing drug (PS), and oxygen to kill microorganisms selectively [5]. The PS accumulates in the microbial cells and then is activated by the light. In the presence of oxygen, this activation generates reactive oxygen species (ROS), which induce oxidative damage to cellular structures, ultimately leading to microorganism death [4]. This therapeutic modality could be useful in situations in which conventional antimicrobial agents may be limited or ineffective, offering a potential alternative for the treatment of localized infections without the risk of drug resistance development [6].

Additionally, recent advances in nanotechnology have positioned it as a cutting-edge tool for enhancing antimicrobial strategies. Engineered nanoparticles (NPs) have been explored for their dual role in this field. As drug delivery systems, they act as carriers for chemotherapeutics improving targeted delivery, bioavailability, and controlled release [7–9] Additionally, certain NPs possess intrinsic antimicrobial properties, either by generating ROS [10], disrupting microbial membranes [10], or interfering with essential cellular functions [11].

In PDI, nanoplatforms can be designed to carry PSs, thereby enhancing their solubility, stability, and bioavailability [12, 13]. Additionally, NPs can directly modulate the interaction between PSs and light, increasing ROS production and improving the overall efficacy of the treatment [14]. Furthermore, a distinct class of nanostructures, known as upconversion and downconversion NPs, leverages the phenomenon of light wavelength transformation (for shorter and longer wavelengths, respectively) upon NP interaction to generate light at wavelengths specifically suited for exciting the PS [15].

As the field of nanotechnology advances, the association of NPs and PDI represents a realistic promise on the horizon. This combination could pave the way for more efficient and targeted treatment strategies against fungal infections. Herein, we systematically searched the global scientific literature to gather evidence of the effects of PDI combined with NPs against the WHO fungal priority pathogens.

2 Methodology

This systematic review adhered to the Preferred Reporting Items for Systematic Reviews (PRISMA) statement [16]. We outlined the criteria for population, intervention, control, and outcome (PICO) to address the specific question "Can engineered NPs improve PDI of priority fungi?", where P denotes fungal burden, I represents PDI associated with NPs, C signifies control PDI, and O indicates reduction of fungal load.

The search spanned 2008 to February 2025, utilizing Embase, Pubmed, Scopus, and Web of Science databases. Keywords related to WHO priority fungi, PDI, and nanotechnology were employed using Boolean operators AND/OR to refine the search, which included: (Nano* OR Liposome, which capture a broad range of nanotechnology-based approaches, including nanoparticles, nanomaterials, nanoplatforms, nanostructures, nanosystems, and liposomal formulations) AND (Photosensitization OR Photodynamic OR Photoinactivation, which ensure the inclusion of studies related to PDI) AND (*Candida* OR *Aspergillus* OR *Cryptococcus* OR *Nakaseomyces* OR *Histoplasma* OR *Eumycetoma* OR *Mucorales* OR *Fusarium*, which specifically target critical and high WHO-listed priority fungi, which are: i-) Critical priority group: *Aspergillus fumigatus, Candida albicans, Candida auris, and Cryptococcus neoformans*; ii-) High priority group: *Histoplasma* spp., *Eumycetoma* causative agents, *Mucorales*, *Nakaseomyces glabrata* (*Candida glabrata*), *Fusarium* spp., *Candida tropicalis*, and *Candida parapsilosis*.

The study selection included original articles and conference proceedings on interventions in in vitro studies published in English, ensuring the inclusion of relevant unpublished or early-stage research. This approach helps mitigate publication bias while maintaining a focus on high-quality, peer-reviewed sources. Thus, we removed duplicates and excluded reviews, letters, comments, abstracts, and articles published in languages other than English. Additionally, studies involving in vivo experimentation, thermal effects of NPs, and NPs serving solely as a PS or as an antimicrobial agent were also excluded from consideration.

Screening of titles and/or abstracts retrieved by the search was conducted using a Microsoft Excel spreadsheet, including author information, journal, and year of publication. For inclusion, studies were required to exhibit consistent NP + PS characterization, with NPs having a size of below 250 nm. Indeed, NPs are typically defined as having dimensions between 1 and 100 nm. However, their hydrodynamic size measured by dynamic light scattering (DLS) is often larger than the size observed by transmission electron microscopy (TEM) due to factors such as aggregation and surface hydration [17]. To account for this aspect and avoid excluding relevant studies, we set the cut-off at 250 nm based on DLS measurements, ensuring that NPs within the conventional nanoscale range (as observed in TEM) were not unintentionally omitted. Additionally,

they were expected to feature a PDI control group with PS alone and target fungal strains classified as high and critical priority by the WHO.

Studies were excluded if they reported PDI combined with another therapeutic strategy, such as chemotherapy, phytotherapy or thermal therapy, a reduction in colony-forming units/mL (CFU/mL) of planktonic yeast cells by less than 3 $\log_{10}$ (99.9%), as this level of reduction would not be considered fungicidal [18], and lack PDI parameters, including PS concentration, light source wavelength, and irradiation parameters such as light dose, irradiance, and/or exposure time. Indeed, eligible articles should provide sufficient information regarding the light source to enable the calculation of light parameters.

All authors contributed to assessing study eligibility, resolving disagreements through discussion and consensus. This collaborative approach ensured a thorough evaluation and minimized subjective bias in study selection.

3 Results

A total of 879 studies were initially identified across the databases. After removing duplicates, 431 studies were screened based on their titles and abstracts, leading to the exclusion of 448 studies. Subsequently, 54 articles were assessed for eligibility, and 10 studies met the inclusion criteria for this review (Fig. 1).

Most investigations were conducted on *Candida albicans* planktonic cells [19–27], with four studies assessing *C. albicans* biofilms [19, 21, 23, 28]. Additionally, there was one study focused on *Fusarium keratoplasticum* [25]. Five studies involved the use of metallic NPs [21, 22, 25–27], while one study reported superparamagnetic iron oxide nanoparticles (SPIONs) to mediate PDI [24]. The remaining four studies encompassed polymeric NPs such as chitosan (CS) [19], micelles [28], polylactic acid (PLA) NPs [23], and cellulose nanocrystals (CNC) [20]. Table 1

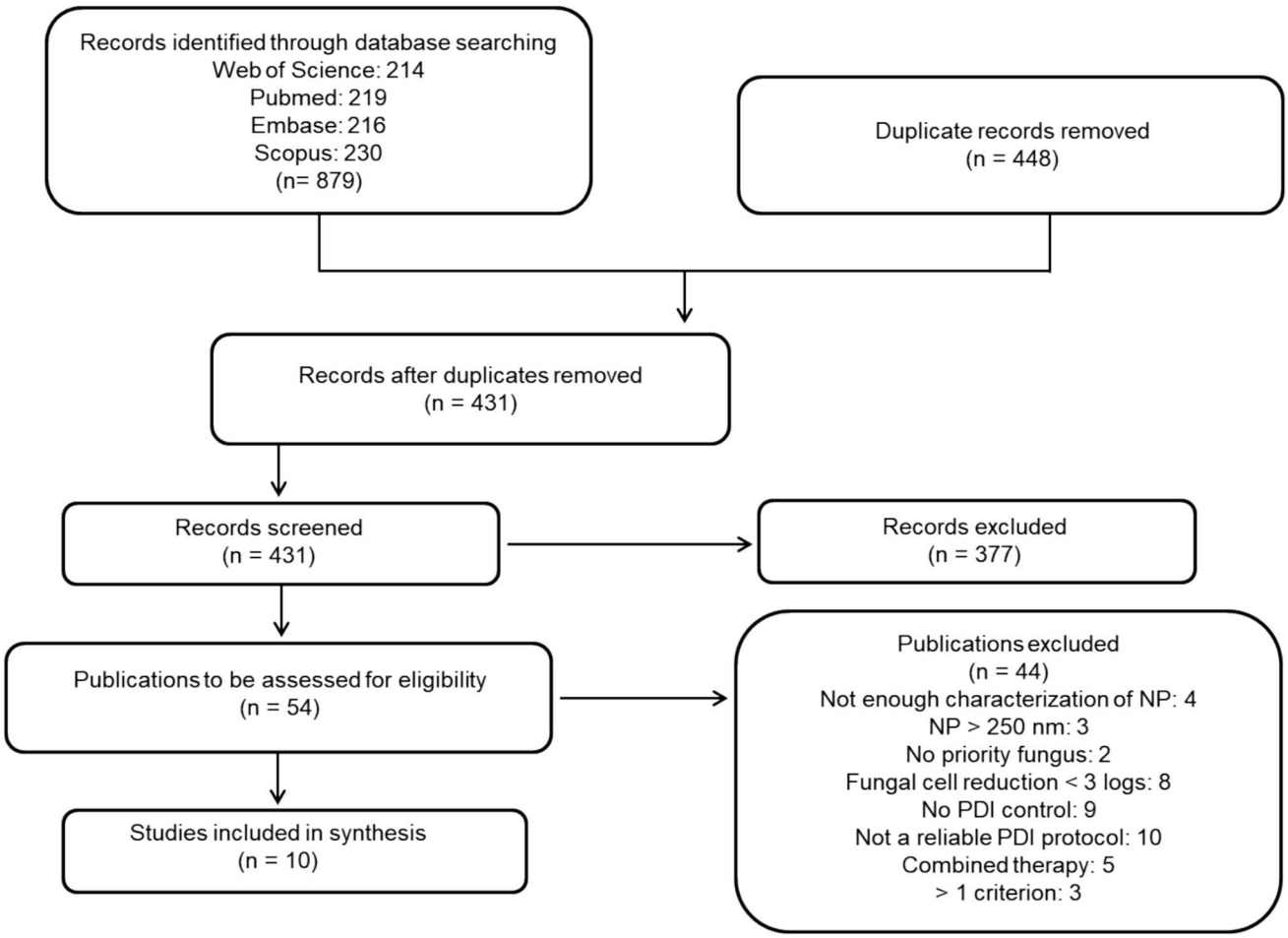

Fig. 1 Flowchart of the paper selection process for the systematic literature review conducted following PRISMA guidelines [16]. A total of 879 studies were initially retrieved, and 448 duplicate records were removed. Next, 431 publications were screened, and 54 full-text articles were evaluated for eligibility. After that, 44 studies were removed, resulting in 10 studies included in the review

lists the fungal species assessed in each study, with characterization of nanoparticles, including their type, shape, and average size. It also displays the peak of the ultraviolet–visible (UV–Vis) spectrum for the nanostructures and/or the PS alone.

Table 2 shows the optimal photoinactivation protocol for the nanostructures. For PDI, studies reported the use of phenothiazines [25, 27, 28], xanthenes [19, 21], porphyrins [24, 26], curcumin [23], and phthalocyanines [20, 22] as the PS. Different light sources, such as lasers [22, 28], light-emitting diodes (LEDs) [19, 23, 25–27], and lamps [20, 21, 24], were employed based on the peaks of absorbance of the nanostructures and/or PS, as reported in Table 1. Overall, the PS concentration and light parameters varied substantially among the studies.

Metallic NPs can trigger a collective oscillation of electrons within the conduction band, a phenomenon known as localized surface plasmon resonance (LSPR), a distinctive optical feature influenced by their size, shape, and composition [29]. In most studies involving metallic NPs, TEM revealed that they exhibited a spherical morphology [21, 22, 25, 26], while one study showed prismatic NPs [27] (see Table 1). The confirmation of the interaction between the PS and NPs was usually achieved through alterations in Zeta (ζ) potential and/or changes in the absorption spectra of PSs.

Maliszewska et al. used gold NPs (AuNPs), with a plasmon resonance at 535–537 nm and 24 nm of size by TEM, mixed with the xanthene rose bengal (RB), which presents an absorption peak centered at 541 nm [21]. In the study, the authors utilized a wide-band Xe lamp (500–780 nm) with different light doses. Their results demonstrated a clear dose-dependent relationship, in which the highest light dose led to the greatest level of fungal death. Indeed, when RB at a concentration of 12.5 mg/L was employed for PDI of *C. albicans* using a light dose of 95.4 J/cm^2, a reduction of 2.19 $\log_{10}$ was achieved. However, when RB was combined with AuNPs under the same conditions, the reduction increased substantially to 4.89 $\log_{10}$, indicating an enhancement of 2.7 $\log_{10}$. In the context of biofilms, a comparable trend was noticed. RB-mediated PDI resulted in a reduction of 0.6 $\log_{10}$, whereas the combination of RB with AuNPs yielded a reduction of 1.53 $\log_{10}$ (Table 3). According to the authors, the enhanced performance of AuNPs in conjunction with RB for PDI may be attributed to the increased uptake of RB by the cells when combined with AuNPs, which was approximately 13% higher compared to RB alone.

Raposo and colleagues reported the application of silver NPs (AgNPs) measuring 14 nm (estimated by TEM) and displaying a plasmon band around 413 nm, aligned with the absorption band of cationic Zn(II)

Table 1 Fungal species and characterization of NPs. The peak of absorbance UV–Vis corresponds to the nanostructure and/or PS alone

Reference	Fungal species	Type of NP	Shape	Average size (nm)	UV–Vis spectrum peak (nm)
[21]	*C. albicans* (planktonic and biofilm)	Au	spherical	24 ± 3 (TEM)	535–537 (plasmon) 541 (PS)
[22]	*C. albicans* (planktonic)	Au/Ag	spherical	16 ± 3 (TEM) (Au:Ag = 2:1)	513–515 (plasmon) (Au:Ag = 2:1) ~ 340 and 670 (PSs)
[26]	*C. albicans* (planktonic)	Ag	spherical	14 (TEM)	413 (plasmon) ~ 425 (PS)
[25]	*C. albicans* and *F. keratoplasticum* (planktonic)	Ag	mostly spherical	16 to 33 (TEM)	~ 420 (plasmon) 655 (MB) 624 (NMBN) 627 (NMBN-Zn)
[27]	Fluconazole-resistant *C. albicans* (planktonic)	Ag	prismatic	37 ± 8 (TEM)	664 (plasmon and PS)
[24]	*C. albicans* (planktonic)	SPIONs	spherical	12 ± 2 (TEM)	~ 430 (nanosystem) ~ 410 (PS)
[19]	*C. albicans* (planktonic and biofilm)	Chitosan	irregular shape	80.9 ± 7.43 (DLS)	Not reported
[23]	*C. albicans* (planktonic and biofilm)	PLA	spherical	Anionic: 193 (FEG-SEM) Cationic: 214 (FEG-SEM)	425–429 (NP and PS)
[20]	*C. albicans* (planktonic)	CNC	rod-shaped	CNC-1: 234 ± 17 (DLS)	670 (CNC- 1) (NP and PS)
[28]	*C. albicans* (biofilm)	Micelles	spherical	25.8 ± 1.8 (DLS)	Not reported

TEM Transmission Electron Microscopy, *SPIONs* Superparamagnetic Iron Oxide Nanoparticles, *DLS* Dynamic Light Scattering, *PLA* Polylactic Acid, *CNC* Cellulose Nanocrystal, *FEG-SEM* Field Emission Gun Scanning Electron Microscopy, *MB* Methylene blue, *NMBN* New methylene blue N, *NMBN-Zn* New methylene blue N Zinc, *Au* Gold, *Ag* Silver

Table 2 Best photoinactivation protocol for the nanostructures

Reference	Photosensitizer (PS)	PS concentration with nanoparticle	Dark period (min)	Light source and λ (nm)	Power density (mW/cm^2)	Light dose (J/cm^2)	Exposure Time (min)
[21]	RB	12.5 mg/L	120	Xe Lamp (500–780)	53	95.4	30
[22]*	$AlPcS_2$ and $AlPcS_3$	7 mg/L	30	Laser (650)	105	63 ($AlPcS_2$) 94.5 ($AlPcS_3$)	10 15
[26]&	ZnPH ZnPE	0.2 µM (ZnPH) 0.6 µM (ZnPE)	10	LED (410 ± 20)	24.1	4.3	3
[25]#	MB, NMBN, and NMBN-Zn	*C. albicans* MB: 0.39 µg/mL NMBN: 0.21 µg/mL NMBN-Zn: 0.13 µg/mL *F. keratoplasticum* MB: 0.79 µg/mL NMBN: 0.10 µg/mL NMBN-Zn: 0.26 µg/mL	30	LED (600–650; λ_{max} = 635)	15.23	15	16.4
[27]	MB	50 µM 100 µM	30	LED (660)	45.9	5 11	2 4
[24]	$TPPF_{20}$	2 µM	30	Lamp (350–800)[a]	90	162	30
[19]	ER	0.88 mg/mL (planktonic) 1.76 mg/mL (biofilm)	120 (planktonic) 1440 (biofilm)	LED (540 ± 5)	22	50	37.9[b]
[23]	CUR	130 µM (planktonic) 260 µM (biofilm)	40 min	LED (440–460, λ_{max} = 455)	33.58	43.2	20
[20]	ZnPc	3 µM	-	Red light (620–645)	18	64	60[b]
[28]	MB	780 µM	30	Laser (660)	19	15	13.2

[a]reported in Ferreira et al., J. Photobiochem Photobiol B. 158: 243–251, 2016

[b]calculated by reviewers

*Molar ratio of Au:Ag = 2:1. & For PDI alone, ZnPH and ZnPE were used at 0.8 µM and 5 µM, respectively. # In PDI alone, the PS concentrations were as follows: MB (1.59 and 1.59 µg/mL), NMBN (0.43 and 0.21 µg/mL), and NMB-Zn (0.52 and 0.26 µg/mL), for *C. albicans* and *F. keratoplasticum*, respectively

N– 2-alkylpyridylporphyrins (ZnTnHex-2-PyP^{4+} and ZnTE-2-PyP^{4+}, ZnPH and ZnPE, respectively) in PDI of *C. albicans* yeasts [26]. The authors investigated the combined use of both ZnPH and ZnPE with AgNPs, exploring different ratios of AgNPs:ZnP (1:4 or 4:1 v/v). The assays were carried out under irradiation with a blue LED (peak at 410 nm). In their study, PDI mediated solely by ZnPH (0.8 µM) or ZnPE (5 µM) on *C. albicans* with a light dose of 4.3 J/cm^2, achieved reductions of approximately 3 $\log_{10}$ and 2 $\log_{10}$, respectively. When the AgNPs-ZnP systems were applied at different ratios under the same light dose, an optimization in PDI was observed. Particularly, the AgNPs-ZnPH systems demonstrated effectiveness at remarkably low PS concentrations, achieving complete inactivation at 0.2 µM. Similarly, AgNPs-ZnPE at 0.6 µM showed effective eradication of yeast cells in both proportions of AgNPs (Table 3). These findings were credited to the increased production of ROS when AgNPs were incorporated into the system, as observed in the ROS evaluation assay, and an enhanced PS-cell interaction provided by the nanostructures, as noted in microscopy analyses.

The PDI involving two types of tetrapyrrole macrocycles compounds, namely di- and trisulfonated hydroxyaluminum phthalocyanines ($AlPcS_2$ and $AlPcS_3$, respectively), associated with Au/Ag bimetallic alloys NPs (prepared in different proportions Au:Ag = 2:1, 1:1, and 1:2), was evaluated by Maliszewska and colleagues [22]. The nanostructures exhibited different sizes according to Au:Ag proportion, which varied from 5 to 22 nm according to TEM results. Although PSs presented Soret and Q absorption bands centered around

Table 3 Fungal killing under the conditions reported in Table 2

Reference	Fungal killing (PDI)	Fungal killing (PDI + NP)
[21]	2.39 $\log_{10}$ (planktonic) 0.6 $\log_{10}$ (biofilm)	4.89 $\log_{10}$ (planktonic) 1.53 $\log_{10}$ (biofilm)
[22]	< 1 $\log_{10}$ ($AlPcS_2$) < 1 $\log_{10}$ ($AlPcS_3$)	Eradication ($AlPcS_2$) 5 $\log_{10}$ ($AlPcS_3$)
[26]	3 $\log_{10}$ (ZnPH) 2 $\log_{10}$ (ZnPE)	Eradication*
[25]	*C. albicans* 3 $\log_{10}$ (MB and NMBN) 5 $\log_{10}$ (NMBN-Zn) *F. keratoplasticum* 3 $\log_{10}$ (MB) 2.5 $\log_{10}$ (NMBN) 3.5 $\log_{10}$ (NMBN-Zn)	*C. albicans** 3 $\log_{10}$ (MB) 4 $\log_{10}$ (NMBN) 4.5 $\log_{10}$ (NMBN-Zn) *F. keratoplasticum** 3 $\log_{10}$ (MB) 4 $\log_{10}$ (NMBN and NMBN-Zn)
[27]	1 $\log_{10}$	Eradication
[24]	< 1 $\log_{10}$	3.7 $\log_{10}$[a]
[19]	3 $\log_{10}$ (planktonic) No reduction (biofilm)	Eradication (planktonic)[b] ~ 3.5 $\log_{10}$ (biofilm)
[23]	Eradication (planktonic) 2.26 $\log_{10}$ (biofilm)	Planktonic: < 1 $\log_{10}$ (anionic NP) Planktonic: Eradication (cationic NP) Biofilm: No reduction (anionic NP) Biofilm: 2 $\log_{10}$ (cationic NP)[#]
[20]	No reduction	6.5 $\log_{10}$[c]
[28]	< 1 $\log_{10}$	Eradication

[a]when both NPs and PS were positively charged

[b]when the volume ratio of chitosan to the ionic gelator was 5:1

[c]when the cellulose nanocrystal was less hydrophilic (CNC-1)

*At lower PS concentrations than PDI alone

[#]Free cationic NPs in the dark showed similar results to PDI alone

340 nm and 670 nm, respectively, distinct plasmon band profiles were in accordance with the bimetallic alloy ratios employed: 513–515 nm (Au:Ag = 2:1), 505–509 nm (Au:Ag = 1:1), and 486–489 nm (Au:Ag = 1:2). The authors used a 650 nm diode laser at various light doses on *C. albicans* planktonic cells, combining $AlPcS_2$ and $AlPcS_3$ at 7 mg/L with different Au:Ag proportions. Cell viability demonstrated a dependence on light dose. At the highest light dose of 94.5 J/cm^2, a reduction lower than 1 $\log_{10}$ was observed when PSs were applied alone. When NPs were used at different Au:Ag ratios, PDI achieved better results than PS alone. Interestingly, PSs combined with NPs at the highest Au concentration exhibited the best PDI performance (Au:Ag = 2:1 ratio). Indeed, a complete eradication of fungal cells was observed for $AlPcS_2$ at a light dose of 63 J/cm^2, while a reduction of approximately 5 $\log_{10}$ was reached for $AlPcS_3$ at 94.5 J/cm^2 (Tables 2 and 3).

Caruso and colleagues utilized AgNPs in PDI of both *C. albicans* and *F. keratoplasticum* cells. In their study, they employed three phenothiazines: MB, new MB N (NMBN), and new MB N formula with zinc (NMBN-Zn) [25]. The AgNPs were predominantly spherical, with a mean size ranging from 16 to 33 nm by TEM. The AgNP-PS association showed the presence of AgNPs by the altered plasmon band around 420 nm with an absorption peak according to the PS (MB: 655 nm; NMBN: 624 nm; NMBN-Zn: 627 nm). The authors determined the minimum inhibitory concentration (MIC) at various light doses delivered by a red LED with a peak at 635 nm for the three PSs. At the highest light dose (15 J/cm^2), the nanosystems incorporating NMBN and NMBN-Zn demonstrated approximately a 4 $\log_{10}$ and 4.5 $\log_{10}$ reduction in *C. albicans*, respectively, with a PS concentration at least two times lower than the MIC for PS in its free form. A similar profile was observed for *F. keratoplasticum*. For this species, PDI mediated by MB in its free form (MIC = 1.59 µg/mL) showed a similar reduction to PDI mediated by the nanosystem, in which MB was used at 0.79 µg/mL (Tables 2 and 3).

Rodrigues and collaborators prepared silver prismatic nanoplatelets (AgNPRs) and decorated them with MB at three different concentrations (25, 50, and 100 µM) [27]. The AgNPRs had a mean size of 37 ± 8 nm (TEM) and a plasmon peak at 664 nm, which matched the absorbance of MB. They used a red LED (660 nm) and varied both MB concentration and exposure time (0 to 240 s) to explore the effects of PDI on fluconazole-resistant *C. albicans*. Their results revealed that PDI alone (MB at 100 µM) was able to kill approximately 1 $\log_{10}$ cells. When PDI was mediated by

AgNPRs, fungal inactivation depended on both MB concentration and light dose. The higher the concentration of MB and the dose of light, the greater the fungal killing. AgNPRs eradicated fungal cells after 240 s and 120 s of irradiation when MB was used at 50 and 100 µM, respectively (Tables 2 and 3). The authors suggested that AgNPRs boosted MB photoactivity through plasmonic effect and by minimizing MB dimerization.

Scanone et al. developed nanoplatforms using derivatives of 5,10,15,20-tetrakis (pentafluorophenyl) porphyrin ($TPPF_{20}$) covalently linked to silica-coated SPIONs, with an average particle size of 12 nm as determined by TEM [24]. Four conjugates were obtained through in situ modifications, two of them without intrinsic net charges and two with cationic groups. After the covalent binding of $TPPF_{20}$, small changes in ζ potential values, absorption and fluorescence spectra, were observed compared to free PS. In the PDI experiments, cultures of *C. albicans* were exposed to visible light (350–800 nm) at different light doses. The inactivation achieved with 2 µM $TPPF_{20}$ was less than 1 $\log_{10}$. Conversely, all conjugates exhibited a greater reduction in a dose-dependent manner, with the conjugate in which both the porphyrin and NP were cationic, achieving a reduction of 3.7 $\log_{10}$ at 162 J/cm^2 (Tables 2 and 3).

CS NPs, when loaded with erythrosine (ER) (CS-ERNPs), showed particle average size varying between 75.3 nm and 266.2 nm by DLS, depending on the concentration of CS, ER, and sodium tripolyphosphate (TPP), which acted as an ionic gelator for CS [19]. Microbiological assays were carried out with the formulation in which the CS/TPP volume ratio was 5/1, as this ratio showed the most significant binding of ER to cells. The CS-ERNPs were evaluated in different dark incubation periods (10 min, 2 h, 12 h, or 24 h) before exposure to green light (540 ± 5 nm) with different light doses. The CS-ERNPs were more effective against *C. albicans* than free ER at the same concentration (0.88 mg/mL). Complete eradication of planktonic cells was achieved after a 2-h incubation with the nanosystem, followed by exposure to 50 J/cm^2 of light, while treatment with ER alone resulted in a reduction of 3 $\log_{10}$. For biofilms, free ER (1.76 mg/mL, 24 h incubation, 50 J/cm^2) showed no reduction, while PDI mediated by CS-ERNPs resulted in a decrease of ~ 3.5 $\log_{10}$ (Table 3).

Trigo Gutierrez et al. developed curcumin (CUR)-loaded polymeric NPs (prepared with polylactic acid, PLA), which exhibited regular size and shape but different charges. The size and the ζ potential varied over time (0 to 40 days) [23]. Anionic CURNPs (only PLA) presented a mean size of 193 nm while cationic CURNPs, in which CTAB was used as a surfactant, exhibited a mean size of 214 nm as measured by Field Emission Gun Scanning Electron Microscopy (FEG-SEM). For PDI, the authors employed an LED with λ_{max} = 455 nm delivering a light dose of 43.2 J/cm^2. They observed that irradiated free CUR (130 µM) eliminated *C. albicans* yeasts. Anionic CURNPs caused a reduction in yeasts of 0.78 $\log_{10}$, whereas cationic CURNPs, with or without light, eradicated *C. albicans*, indicating intrinsic fungicidal effects. In biofilms, free CUR (1200 µM) reduced the fungal load by 2.26 $\log_{10}$. Anionic CURNPs showed limited effects, while cationic NPs (both free and CUR-loaded) promoted a reduction of approximately 2 $\log_{10}$ at a CUR concentration of 260 µM (Table 3). The authors attributed the cytotoxicity observed in cationic formulations to CTAB while they linked the cytotoxic effect of free CUR to the high DMSO concentration.

Anaya-Plaza et al. described novel nanostructures resulting from the immobilization of cationic derivatives of zinc phthalocyanine (ZnPc) on unmodified cellulose nanocrystals (CNCs) [20]. The chosen ZnPc compounds feature eight pyridinium moieties, which were covalently linked to two CNCs that differed in hydrophilicity. Only the less hydrophilic compound (CNC-1) was tested for antifungal PDI of *C. albicans* cells. CNC-1 loaded with ZnPc showed an average size of 234 nm as analyzed by DLS. They employed red light (620–645 nm) at different light doses. CNC-1 demonstrated greater efficacy without toxicity in the dark, achieving a reduction of 6.5 $\log_{10}$ at 3 µM (Table 3). In contrast, its free form showed no significant effects for the highest light dose of 64 J/cm^2. According to the authors, the low activity of free ZnPc may be attributed to strong aggregation, hindering its interaction with cells.

Polymeric-neutral micelles prepared from Pluronic®F-127 and loaded with MB at 780 µM were investigated by Soares et al. [28]. These micelles exhibited a particle mean size of 25.8 nm (from DLS), a spherical shape, and a neutral surface charge that maintained stability for 90 days. The efficacy of these systems was evaluated against biofilms formed within 48 h by *C. albicans* under different periods of dark incubation, red laser (λ = 660 nm), and dose of 15 J/cm^2. Overall, the results showed that biofilm disruption depends on the period in dark incubation, with a complete fungal reduction observed for 30 min of incubation in the dark before irradiation. Free MB-mediated PDI showed a decrease of 1 $\log_{10}$ (Table 3).

4 Discussion

Infections caused by WHO's priority fungi represent a significant public health challenge. These fungi are prioritized based on their impact, the severity of associated diseases, and the challenges they present in diagnosis and treatment. Factors such as the increasing use of immunosuppressive therapies, widespread use of antimicrobials, global travel, and climate change can contribute to the rise of these infections [30]. Therefore, there is an urgent need for the

development of effective treatment strategies to tackle these infections. Consequently, systematic reviews could play a pivotal role in elucidating the advantages, obstacles, and constraints associated with the proposed treatment protocols for fungal infections.

To our knowledge, we conducted the first systematic review aimed at investigating whether engineered NPs could improve PDI against the WHO fungal priority pathogens. The main goal of this study was to establish whether robust scientific evidence exists to support the potential of this associated therapy in combating these medically important pathogens, which could open new avenues of knowledge and inspire further clinical studies.

We noticed that 26 studies did not report either sufficient NP characterization or complete PDI protocol (see Fig. 1). This finding highlights the importance of rigorous methodologies for future studies. Additionally, we identified studies against only two species from the WHO fungal priority list, which are ranked as critical (*C. albicans*) and high (*F. keratoplasticum*) priority pathogens. Most studies investigated the association of PDI and NPs against *C. albicans* in planktonic cells.

The *Candida* genus encompasses various species, some of which are commensal organisms inhabiting the human body, while others can cause opportunistic infections, particularly in immunocompromised individuals [2]. From a clinical standpoint, candidiasis poses significant challenges to public health due to its increasing prevalence and resistance to antifungal treatments. *C. albicans* exhibits a remarkable ability to develop resistance to commonly used antifungal agents, including azoles (*e.g.,* fluconazole, itraconazole, ketoconazole, and miconazole), due to the widespread use of these medications [3].

Antifungal resistance in *C. albicans* is a complex issue that extends beyond simple genetic mutations, involving a variety of adaptive strategies the organism uses to evade the effects of these drugs [21]. Key resistance mechanisms include the upregulation of drug efflux pumps, such as ABC and MFS transporters, which actively expel antifungal drugs from the cell, thereby reducing their efficacy [31]. Additionally, alterations in the drug's target sites, such as mutations in the lanosterol 14α-demethylase enzyme, can decrease the binding affinity of azoles, rendering them ineffective [32]. Biofilm formation is another critical factor, as *C. albicans* can form protective biofilms that limit drug penetration and shield the organism from immune response [33]. The ability to efficiently adapt its metabolic pathways allows *C. albicans* to survive under drug stress by utilizing alternative energy sources, further enhancing resistance [34]. The organism also exhibits increased genetic plasticity, including chromosomal rearrangements and aneuploidy, which enable rapid adaptation to antifungal pressure [34]. Moreover, cross-resistance and multidrug resistance can occur, where resistance to one antifungal class leads to a reduced effectiveness of other drugs, significantly complicating treatment options [34]. These mechanisms collectively present a major challenge in treating *C. albicans* infections, highlighting the need for novel therapeutic strategies and improved antifungal management.

Recent studies have also highlighted the potential role of *C. albicans* interaction with the human microbiome in its pathogenicity and resistance mechanisms [35, 36]. This interaction not only contributes to its ability to thrive in host environments but may also complicate treatment efforts [37]. While further research is needed to investigate the factors derived from *C. albicans* and the host immune system that regulate the shift between commensalism and pathogenicity, understanding these dynamics presents new challenges and opportunities for developing more targeted and effective therapeutic strategies.

Fusarium species also present substantial clinical challenges, particularly in the context of invasive fusariosis, a life-threatening condition with mortality rates ranging from 43 to 67% [3]. This high mortality has been attributed to the inherent resistance of *Fusarium* spp. to many available antifungal agents, limiting treatment options [1]. The complex resistance mechanisms, including its ability to form biofilms, its propensity to cause severe disseminated infections, especially in immunocompromised individuals, and the increasing trends over the last 10 years, highlight the importance of this species as a global priority pathogen. Hence, the development of novel therapeutic strategies that address the challenges posed by *Candida* and *Fusarium* infections, in addition to the other WHO priority fungi, is crucial.

It is worth noting that other studies reporting critical priority fungi, such as *C. neoformans*, did not meet our inclusion criteria. Further research could encompass other critical priority fungi, such as *C. auris*, a superbug currently of significant concern [38]. Remarkably, *C. auris* has been recognized as a global public health threat emerging in healthcare settings, representing a red-alert situation due to its high resistance to multiple classes of antifungal drugs, including azoles, echinocandins, and polyenes [38, 39]. This multidrug resistance profile makes *C. auris* infections difficult to treat, complicating clinical outcomes and potentially increasing mortality rates [39]. Additionally, *C. auris* can persist on surfaces and spread rapidly within hospital environments, leading to outbreaks among vulnerable patient populations, particularly those with weakened immune systems or invasive medical devices [40]. The rising incidence of *C. auris* infections, combined with the limited availability of novel antifungal therapies, highlights the need for alternative treatments, such as PDI combined with NPs, which could offer a promising avenue for further investigation.

PDI offers notable advantages against fungal infections, however, this strategy also presents limitations that hinder

its overall effectiveness. Intrinsic properties of PSs, including their ionic and lipophilic character as well as chemical stability, can reduce their efficiency in producing ROS near cellular structures for optimal performance in PDI [6]. In addition, fungal defense mechanisms, such as reduction in PS uptake due to efflux pumps and the upregulation of antioxidant enzymes like catalase and superoxide dismutase, can neutralize ROS [21]. Yet, the penetration of the PS may be hampered by limited diffusion through the extracellular matrix composed of polysaccharides or by genotypic and phenotypic alterations.

Nanotechnology rises in this context to improve PDI, enhancing the effectiveness and versatility of the treatment. In this review, metallic NPs were used to enhance PDI of various classes of PSs, such as xanthenes [21], phthalocyanines [22], porphyrins [26], and phenothiazines [25, 27], which displayed absorption peaks across diverse spectral regions. For these nanostructures, Maliszewska and colleagues demonstrated that *C. albicans* cells exhibited increased internalization of RB and phthalocyanines when conjugated with spherical AuNPs or Au/AgNPs, respectively, compared to their free forms [21, 22]. Similarly, Raposo et al. [26] observed enhanced cellular uptake of two zinc porphyrins when associated with spherical AgNPs. Rodrigues et al. [27] reported that AgNPRs have the capacity to facilitate the reduction of MB aggregation. It seems that metallic NPs serve as nanocarriers, aiding in the penetration/retention intracellular of PSs, consequently resulting in higher rates of cell death. It is also important to highlight that LSPR has the capability to enhance the electromagnetic field in the vicinity of the NP if the plasmon band is resonant with the PS absorption band [41], thereby amplifying PS excitation and subsequently increasing the production of ROS, as observed by Raposo and colleagues [26].

The design of NPs for delivering PSs employs various strategies tailored to the unique properties of the nanomaterials used. Because of their distinctive magnetic properties, SPIONs offer the advantage of coupling a PS and using an external magnetic field as a guide. Scanone et al. reported that SPIONs coated with silica have the potential to serve as effective nanocarriers for the porphyrin $TPPF_{20}$, improving PDI [24]. Surprisingly, after PDI, SPIONs were recovered using magnetic decantation and reused in subsequent PDI cycles, demonstrating consistent efficiency even after three cycles. It is promising to envision a future in which nanomaterials could be employed to precisely target and deliver PSs to internal infectious sites.

We found compelling evidence indicating that polymeric NPs used for transporting PSs can be derived from biopolymers such as CS [19] and cellulose [20]. These biomaterials provide a variety of shapes, natural abundance, and reduced risk of toxicity. The incorporation of PSs into nanostructures can be achieved through surface modifications that introduce cationic or anionic characteristics. These findings suggest that biopolymeric NPs enhance the delivery of ZnPc and ER with the sustained presence of PSs within cellular structures of *C. albicans*, which contributes to improving the effectiveness of PDI.

CUR is a natural PS with an absorption spectrum in the blue region. However, its hydrophobic nature limits its applications. An alternative approach involves encapsulating CUR in PLA [23]. It seems that cationic CURNPs, whether irradiated or not, can eliminate planktonic cells of *C. albicans* and exhibit an enhanced anti-biofilm effect compared to control and anionic CURNPs. The observed toxicity, however, seemed to be caused by the surfactant (CTAB). On the other hand, although MB is a hydrophilic PS, its encapsulation in polymeric micelles for drug delivery enhanced its antimicrobial activity against *C. albicans*. This improvement was due to increased permeation into biofilms and prolonged PS release [28].

A class of NPs whose studies did not meet our inclusion criteria are those involving the upconversion phenomenon. In this process, the NP can absorb low-energy photons from the near-infrared region, which penetrates deeper into biological tissues [*e.g.*, $LiYF_4$:Yb,Er NP, which is composed of yttrium lithium fluoride ($LiYF_4$) doped with ytterbium (Yb) and erbium (Er) ions] [15]. The energy is sequentially transferred to higher energy levels within the NP and then released as a higher-energy photon, which excites the PS. This mechanism opens new approaches to treating deeper invasive fungal infections, potentially enhancing the PDI efficacy in otherwise challenging conditions.

Overall, based on the studies compiled in this review, advantages of combining PDI with NPs, include: i-) NPs can enhance the solubility of PSs by carrying hydrophobic compounds [20]; ii-) NPs may improve the chemical stability of PSs avoiding aggregation, which could reduce the PS performance [27]; iii-) NPs can be engineered to reduce the required PS concentration for effective fungal elimination [25, 26]; and iv-) Metallic NPs can improve the photophysical properties of PSs, such as enhancing the generation of ROS by LSPR [26]. These attributes could enhance the effectiveness of PDI in treating infections caused by the WHO fungal priority pathogens.

Interestingly, only 4 studies have investigated PDI assisted by NPs in biofilms [19, 21, 23, 28], highlighting a lack of research in more complex biological systems. Except for the study by Trigo Gutierrez et al. [23], all studies reported significantly enhanced fungal killing when the PS was associated with NPs. We assume that NPs may improve PS permeation into biofilms, as reported elsewhere [42]. Our results further support the need for in vivo studies to validate the potential of nanostructure-mediated APDT. NPs can enhance PS uptake by cells, potentially overcoming resistance mechanisms, as observed in tumor cells [43]. These

investigations could help improve the efficacy of APDT against fungal infections.

5 Conclusion

In summary, we present, as far as our knowledge goes, the first systematic review to verify whether engineered NPs can improve PDI against the most medically important fungal pathogens. Our findings revealed a broad range of NPs and PSs used in combination to effectively inactivate *Candida* and *Fusarium* species in vitro. We conclude that NPs could be used to improve fungal inactivation and carry PSs to the infection site, optimizing PDI protocols. More studies are needed to investigate this association, which will enhance our understanding and allow us to expand the research to other WHO priority fungi. Finally, there are few studies using animal models and no clinical trials, highlighting the need to extend this research beyond laboratory benchmarks.

Acknowledgements GSL and JCB-J thank FACEPE, and ARS and BLR thank FAPESP for their scholarships. PECF, AF and MSR acknowledge the support of CNPq through productivity fellowships.

Authors Contribution All authors equally contributed to this manuscript. All authors were responsible for conceptualization, methodology, writing, and revising the review.

Funding This work was funded by FAPESP (grants # 2018/20226–7 and 2021/14119-6), FACEPE (grant APQ-0573–2.09/18), CNPq (grants # 465763/2014–6 and 440228/2021–2), and CNEN.

Data Availability No datasets were generated or analysed during the current study.

Declarations

Ethical Approval Not applicable.

Consent to Participate Not applicable.

Conflict of Interest The authors declare no competing interests.

References

1. Loh, J. T., & Lam, K. P. (2023). Fungal infections: Immune defense, immunotherapies and vaccines. *Advanced Drug Delivery Reviews, 196*, 114775. https://doi.org/10.1016/j.addr.2023.114775
2. Lu, H., Hong, T., Jiang, Y., Whiteway, M., & Zhang, S. (2023). Candidiasis: From cutaneous to systemic, new perspectives of potential targets and therapeutic strategies. *Advanced Drug Delivery Reviews, 199*, 114960. https://doi.org/10.1016/j.addr.2023.114960
3. World Health Organization. (2022). WHO fungal priority pathogens list to guide research, development and public health action. Available at: https://www.who.int/publications/i/item/9789240060241. Accessed 24 Feb 2025.
4. Wainwright, M., Maisch, T., Nonell, S., Plaetzer, K., Almeida, A., Tegos, G. P., & Hamblin, M. R. (2017). Photoantimicrobials—are we afraid of the light? *The Lancet Infectious Diseases, 17*(2), e49–e55. https://doi.org/10.1016/S1473-3099(16)30268-7
5. Cabral, F. V., dos Santos Souza, T. H., Sellera, F. P., Fontes, A., & Ribeiro, M. S. (2023). Strengthening collaborations at the Biology-Physics interface: Trends in antimicrobial photodynamic therapy. *Biophysical Reviews, 15*(4), 685–697. https://doi.org/10.1007/s12551-023-01066-5
6. Cieplik, F., Deng, D., Crielaard, W., Buchalla, W., Hellwig, E., Al-Ahmad, A., & Maisch, T. (2018). Antimicrobial photodynamic therapy–what we know and what we don't. *Critical Reviews in Microbiology, 44*(5), 571–589. https://doi.org/10.1080/1040841X.2018.1467876
7. Zare-Zardini, H., Soltaninejad, H., Ghorani-Azam, A., Forouzani-Moghaddam, M. J., Mozafri, S., Akhoundi-Meybodi, Z., ... & Jabinian, F. (2022). Investigating the Antimicrobial Activity of Vancomycin-Loaded Soy Protein Nanoparticles. *Interdisciplinary Perspectives on Infectious Diseases*, *2022*(1), 5709999, https://doi.org/10.1155/2022/5709999
8. Darvishi, M., Farahani, S., & Haeri, A. (2021). Moxifloxacin-loaded lipidic nanoparticles for antimicrobial efficacy. *Current Pharmaceutical Design, 27*(1), 135–140. https://doi.org/10.2174/1381612826666200701152618
9. Changsan, N., Atipairin, A., Muenraya, P., Sritharadol, R., Srichana, T., Balekar, N., & Sawatdee, S. (2024). *In Vitro* Evaluation of Colistin Conjugated with Chitosan-Capped Gold Nanoparticles as a Possible Formulation Applied in a Metered-Dose Inhaler. *Antibiotics, 13*(7), 630. https://doi.org/10.3390/antibiotics13070630
10. Annunzio, S. R., de Lima Moraes, B., Assis, M., Barbugli, P. A., de Oliveira, V. H. F. P., Longo, E., & Vergani, C. E. (2025). Antimicrobial activity and biocompatibility of alpha-silver tungstate nanoparticles. *Heliyon*. https://doi.org/10.1016/j.heliyon.2025.e42648
11. Radwan, I. T., El-Sherbiny, I. M., Selim, A. M., & Metwally, N. H. (2024). Design, synthesis of some novel coumarins and their nanoformulations into lipid-chitosan nanocapsule as unique antimicrobial agents. *Scientific Reports, 14*(1), 30598. https://doi.org/10.1038/s41598-024-79861-7
12. Wang, H., Li, X., Li, P., Feng, Y., Wang, J., Gao, Q., ... & Liao, Y. (2025). Uptake of Biomimetic Nanovesicles by Granuloma for Photodynamic Therapy of Tuberculosis. *ACS Omega*, https://doi.org/10.1021/acsomega.4c08127
13. Amin, M. U., Ali, S., Engelhardt, K. H., Nasrullah, U., Preis, E., Schaefer, J., ... & Bakowsky, U. (2024). Enhanced photodynamic therapy of curcumin using biodegradable PLGA coated mesoporous silica nanoparticles. *European Journal of Pharmaceutics and Biopharmaceutics*, *204*, 114503, https://doi.org/10.1016/j.ejpb.2024.114503
14. Awad, M., Barnes, T. J., Joyce, P., Thomas, N., & Prestidge, C. A. (2022). Liquid crystalline lipid nanoparticle promotes the photodynamic activity of gallium protoporphyrin against S aureus biofilms. *Journal of Photochemistry and Photobiology B: Biology, 232*, 112474. https://doi.org/10.1016/j.jphotobiol.2022.112474
15. Zhang, Y., Huang, P., Wang, D., Chen, J., Liu, W., Hu, P., ... & Chen, Z. (2018). Near-infrared-triggered antibacterial and antifungal photodynamic therapy based on lanthanide-doped upconversion nanoparticles. *Nanoscale*, *10*(33), 15485–15495, https://doi.org/10.1039/C8NR01967C
16. Page, M. J., Moher, D., Bossuyt, P. M., Boutron, I., Hoffmann, T. C., Mulrow, C. D., ... & McKenzie, J. E. (2021). PRISMA 2020 explanation and elaboration: updated guidance and exemplars for reporting systematic reviews. *BMJ*, *372*, https://doi.org/10.1136/bmj.n160

17. Altammar, K. A. (2023). A review on nanoparticles: Characteristics, synthesis, applications, and challenges. *Frontiers in Microbiology, 14*, 1155622. https://doi.org/10.3389/fmicb.2023.1155622
18. Franconi, I., & Lupetti, A. (2023). In vitro susceptibility tests in the context of antifungal resistance: Beyond minimum inhibitory concentration in *Candida* spp. *Journal of Fungi, 9*, 1188. https://doi.org/10.3390/jof9121188
19. Chen, C. P., Chen, C. T., & Tsai, T. (2012). Chitosan nanoparticles for antimicrobial photodynamic inactivation: Characterization and *in vitro* investigation. *Photochemistry and Photobiology, 88*(3), 570–576. https://doi.org/10.1111/j.1751-1097.2012.01101.x
20. Anaya-Plaza, E., van de Winckel, E., Mikkilä, J., Malho, J. M., Ikkala, O., Gulías, O., ... & de la Escosura, A. (2017). Photoantimicrobial biohybrids by supramolecular immobilization of cationic phthalocyanines onto cellulose nanocrystals. *Chemistry–A European Journal*, *23*(18), 4320–4326, https://doi.org/10.1002/chem.201605285
21. Maliszewska, I., Lisiak, B., Popko, K., & Matczyszyn, K. (2017). Enhancement of the efficacy of photodynamic inactivation of *Candida albicans* with the use of biogenic gold nanoparticles. *Photochemistry and Photobiology, 93*(4), 1081–1090. https://doi.org/10.1111/php.12733
22. Maliszewska, I., Wanarska, E., & Tylus, W. (2020). Sulfonated hydroxyaluminum phthalocyanine-biogenic Au/Ag alloy nanoparticles mixtures for effective photo-eradication of *Candida albicans*. *Photodiagnosis and Photodynamic Therapy, 32*, 102016. https://doi.org/10.1016/j.pdpdt.2020.102016
23. Trigo Gutierrez, J. K., Zanatta, G. C., Ortega, A. L. M., Balastegui, M. I. C., Sanita, P. V., Pavarina, A. C., ... & Mima, E. G. D. O. (2017). Encapsulation of curcumin in polymeric nanoparticles for antimicrobial Photodynamic Therapy. *PLoS One*, *12*(11), e0187418, https://doi.org/10.1371/journal.pone.0187418
24. Scanone, A. C., Gsponer, N. S., Alvarez, M. G., Heredia, D. A., Durantini, A. M., & Durantini, E. N. (2020). Magnetic Nanoplatforms for in Situ Modification of Macromolecules: Synthesis, Characterization, and Photoinactivating Power of Cationic Nanoiman-Porphyrin Conjugates. *ACS Applied Bio Materials, 3*(9), 5930–5940. https://doi.org/10.1021/acsabm.0c00625
25. Caruso, G. R., Tonani, L., Marcato, P. D., & von Zeska Kress, M. R. (2021). Phenothiazinium photosensitizers associated with silver nanoparticles in enhancement of antimicrobial photodynamic therapy. *Antibiotics, 10*(5), 569. https://doi.org/10.3390/antibiotics10050569
26. Raposo, B. L., Souza, S. O., Santana, G. S., Lima, M. T., Sarmento-Neto, J. F., Reboucas, J. S., ... & Fontes, A. (2023). A novel strategy based on Zn (II) porphyrins and silver nanoparticles to photoinactivate *Candida albicans*. *International Journal of Nanomedicine*, 3007–3020, https://doi.org/10.2147/IJN.S404422
27. Rodrigues, C. H., Silva, B. P., Silva, M. L., Gouveia, D. C., Fontes, A., Macêdo, D. P., & Santos, B. S. (2024). Methylene blue@ silver nanoprisms conjugates as a strategy against *Candida albicans* isolated from balanoposthitis using photodynamic inactivation. *Photodiagnosis and Photodynamic Therapy, 46*, 104066. https://doi.org/10.1016/j.pdpdt.2024.104066
28. Soares, J. C. M., Luiz, M. T., Junior, J. A. O., Besegato, J. F., de Melo, P. B. G., de Souza Rastelli, A. N., & Chorilli, M. (2023). Antimicrobial photodynamic therapy mediated by methylene blue-loaded polymeric micelles against *Streptococcus mutans* and *Candida albicans* biofilms. *Photodiagnosis and Photodynamic Therapy, 41*, 103285. https://doi.org/10.1016/j.pdpdt.2023.103285
29. Mcoyi, M. P., Mpofu, K. T., Sekhwama, M., & Mthunzi-Kufa, P. (2024). Developments in localized surface plasmon resonance. *Plasmonics*, 1–40, https://doi.org/10.1007/s11468-024-02620-x
30. Seidel, D., Wurster, S., Jenks, J. D., Sati, H., Gangneux, J. P., Egger, M., ... & Kontoyiannis, D. P. (2024). Impact of climate change and natural disasters on fungal infections. *The Lancet Microbe*, https://doi.org/10.1016/S2666-5247(24)00039-9
31. Holmes, A. R., Cardno, T. S., Strouse, J. J., Ivnitski-Steele, I., Keniya, M. V., Lackovic, K., ... & Cannon, R. D. (2016). Targeting efflux pumps to overcome antifungal drug resistance. *Future Medicinal Chemistry*, *8*(12), 1485–1501, https://doi.org/10.4155/fmc-2016-0050
32. Lee, Y., Puumala, E., Robbins, N., & Cowen, L. E. (2021). Antifungal Drug Resistance: Molecular Mechanisms in *Candida albicans* and Beyond. *Chemical Reviews, 121*(6), 3390–3411. https://doi.org/10.1021/acs.chemrev.0c00199
33. Atriwal, T., Azeem, K., Husain, F. M., Hussain, A., Khan, M. N., Alajmi, M. F., & Abid, M. (2021). Mechanistic Understanding of *Candida albicans* Biofilm Formation and Approaches for Its Inhibition. *Frontiers in Microbiology, 12*, 638609. https://doi.org/10.3389/fmicb.2021.638609
34. Lopes, J. P., & Lionakis, M. S. (2022). Pathogenesis and virulence of *Candida albicans*. *Virulence, 13*(1), 89–121. https://doi.org/10.1080/21505594.2021.2019950
35. Li, H., Miao, M. X., Jia, C. L., Cao, Y. B., Yan, T. H., Jiang, Y. Y., & Yang, F. (2022). Interactions between *Candida albicans* and the resident microbiota. *Frontiers in Microbiology, 13*, 930495. https://doi.org/10.3389/fmicb.2022.930495
36. Wang, F., Wang, Z., & Tang, J. (2023). The interactions of *Candida albicans* with gut bacteria: A new strategy to prevent and treat invasive intestinal candidiasis. *Gut Pathogens, 15*(1), 30. https://doi.org/10.1186/s13099-023-00559-8
37. Proctor, D. M., Drummond, R. A., Lionakis, M. S., & Segre, J. A. (2023). One population, multiple lifestyles: Commensalism and pathogenesis in the human mycobiome. *Cell Host & Microbe, 31*(4), 539–553. https://doi.org/10.1016/j.chom.2023.02.010
38. Du, H., Bing, J., Hu, T., Ennis, C. L., Nobile, C. J., & Huang, G. (2020). *Candida auris*: Epidemiology, biology, antifungal resistance, and virulence. *PLoS Pathogens, 16*(10), e1008921. https://doi.org/10.1371/journal.ppat.1008921
39. Kim, H. Y., Nguyen, T. A., Kidd, S., Chambers, J., Alastruey-Izquierdo, A., Shin, J. H., ... & Alffenaar, J. W. (2024). *Candida auris*—A systematic review to inform the world health organization fungal priority pathogens list. *Medical Mycology*, *62*(6), myae042, https://doi.org/10.1371/journal.ppat.1008921
40. Gaetano, S., Midiri, A., Mancuso, G., Avola, M. G., & Biondo, C. (2024). *Candida auris* Outbreaks: Current Status and Future Perspectives. *Microorganisms, 12*(5), 927. https://doi.org/10.3390/microorganisms12050927
41. Ribeiro, M. S., de Melo, L. S., Farooq, S., Baptista, A., Kato, I. T., Núñez, S. C., & de Araujo, R. E. (2018). Photodynamic inactivation assisted by localized surface plasmon resonance of silver nanoparticles: In vitro evaluation on *Escherichia coli* and *Streptococcus mutans*. *Photodiagnosis and Photodynamic therapy, 22*, 191–196. https://doi.org/10.1016/j.pdpdt.2018.04.007
42. Han, Z., Li, Y., Zhan, X., Sun, M., Liang, Y., Yuan, M., ... & Li, F. (2025). A versatile nanoplatform with excellent biofilm permeability and spatiotemporal ROS regulation for peri-implantitis treatment. *Theranostics*, *15*(8), 3490, https://doi.org/10.7150/thno.108830
43. Rajaram, J., Mende, L. K., & Kuthati, Y. (2024). A review of the efficacy of nanomaterial-based natural photosensitizers to overcome multidrug resistance in cancer. *Pharmaceutics, 16*(9), 1120. https://doi.org/10.3390/pharmaceutics16091120